

ACTIVE VIBRATION CONTROL OF TERFENOL-D ROD OF GIANT MAGNETOSTRICTIVE ACTUATOR WITH NONLINEAR CONSTITUTIVE RELATIONS

HAO-MIAO ZHOU
YOU-HE ZHOU
XIAO JING ZHENG

Lanzhou University, School of Civil Engineering and Mechanics, Department of Mechanics and Engineering Science, Lanzhou, China
e-mail: zhouyh@lzu.edu.cn

This paper presents a numerical simulation of active vibration control of the Terfenol-D rod of a giant magnetostrictive transducer with nonlinear constitutive relations. In this control system, the goal is to suppress vibration of the displacement at the free end of the rod that is usually connected with a platform. Due to the inherent nonlinear relation among the applied magnetic field, pre-stress, and strain, the extension of the rod is also nonlinear relative to the external applications. Having an analytical nonlinear constitutive model of the Terfenol-D rod proposed by the last author of this paper and the finite element method employed in the deformation analysis, we propose a numerical code to simulate the dynamic behavior of the control system when the negative displacement and velocity control law is utilized to feed back the signals to the actuator. The simulation results display that this control is more effective than other existing control algorithms based on linear constitutive models.

Key word: giant magnetostrictive actuators, nonlinear constitutive model, negative feedback control law, active control of vibration suppression

1. Introduction

In the recent ten and more years, some magnetostrictive materials have been discovered to generate large or giant strains in materials by utilizing the realignment of magnetic moments in response to applied magnetic fields like, for example, in a commercially available magnetostrictive material of Terfenol-D

made of an alloy of terbium, iron, and dysprosium, which may generate a strain much more larger than that of other smart materials. To utilize this significant property, one of potential applications is active control of vibration suppression of platforms by embedding the Terfenol-D rods to support such platforms (Jenner *et al.*, 1994; Nakamura *et al.*, 2000; Zhang *et al.*, 2003; Zhang *et al.*, 2004), since the Terfenol-D rod has some distinct advantages over other smart materials, such as high strain, good magnetomechanical coupling factor, fast response, and the magnetostriction property without changing with time, etc. (Bartlett *et al.*, 2001; Carman and Mitrovic, 1995; Duenas *et al.*, 1996; Pagliarulu *et al.*, 2004).

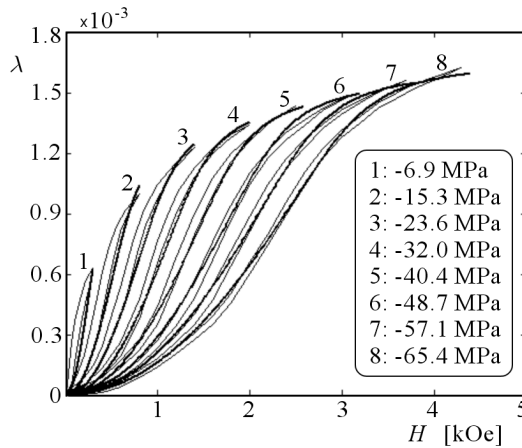


Fig. 1. Comparison of curves of nonlinear magnetostrictive strain versus the magnetic field between experimental measurements (Moffet *et al.*, 1991) and theoretical model (Zheng and Liu, 2005), thin lines: the experimental measurements; bold lines: theoretical predictions

The experimental measurement displayed strong nonlinear behavior of the Terfenol-D rod, i.e. the extension or constriction strain is strongly dependent on the application of both magnetic field and pre-stress, while Young's modulus of the material also changes with its local stress generated in the rod. Figures 1 and 2 show experimental measurements and theoretical results regarding the behavior of a Terfenol-D rod (Moffet *et al.*, 1991; Zheng and Liu, 2005). Due to complexity of constitutive relations in experiments, some theoretical constitutive models have been established only for the case of low magnetic fields and some constants in the models indirectly connected to the existing physical parameters (Carman and Mitrovic, 1995; Duenas *et al.*, 1996). In that case, most control models applying those smart materials were expressed by approximate linearized constitutive relationships of the materials. For

example, Reed (1988) proposed an active control theory for a vibration isolation system of a platform by means of magnetostrictive actuators. Then, Hiller *et al.* (1989) conducted an experiment to show the feasibility of the isolation system using magnetostrictive actuators as support mounts to provide low frequency. In order to control vibration of structures, Flatau and Hall (1992) employed a Terfenol-D actuator as a shaker for active control of vibration. In order to reflect the nonlinear effects of the material, some efforts were made in the simulation of dynamic control systems such as the variable structure algorithm and fuzzy method to compensate these effects (Jenner *et al.*, 1994; Nakamura *et al.*, 2000; Zhang *et al.*, 2003), while the relation between the output displacement and input magnetic field of the actuator was still linear. In fact, these methods are effective only in an approximately linear region of strain-magnetic field curves. It is obvious that the Terfenol-D rod functions as both a sensor (i.e. displacement at the free end) and an actuator in the control system. In such a case, the nonlinear relations of the materials will generate a central role to the control systems.

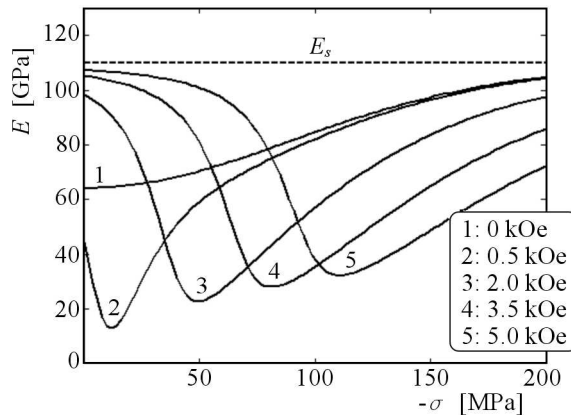


Fig. 2. Curves of Young's modulus versus compressive stress for different bias magnetic fields from the theoretical model (Zheng and Liu, 2005)

Recently, an analytical constitutive model of the Terfenol-D rod has been proposed to fully coincide with experimental measurements, in which the constants in the model were all given by the existing ones (Zheng and Liu, 2005), which provides feasibility of establishing a control theory with practical nonlinear constitutive relations in the control system.

Based on the analytical relations of the nonlinear constitutive model by Zheng and Liu (2005), we propose here a numerical code of an active control system with the Terfenol-D rod with the negative displacement and velocity

feedback control law with constant gain employed. In the simulations, the nonlinear extension of the rod is analyzed by the finite element method for the spatial part, and the Newmark method is employed for the time part, while the nonlinear effect is solved iteratively. After that, the simulation results are displayed to show the efficiency of the proposed control method.

2. Essential formulae for the control system

Here, we consider the control system with a Terfenol-D rod that is subjected to a specific pre-compress stress, a bias magnetic field along its axial direction and an excitation or controlling magnetic field, as shown in Fig. 3. When these

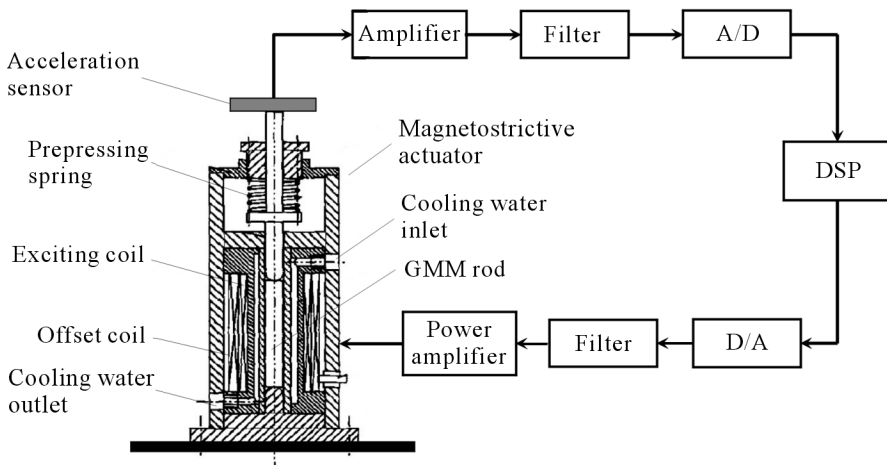


Fig. 3. Schematic drawing of the feedback control system with the Terfenol-D transducer

external conditions are applied to the rod, it generates some extension or contraction. By detecting or sensing the displacement and velocity at the free end of the rod and amplifying the signals of the displacement and velocity, then feeding back the amplified signals back to the controlling magnetic field, a control system for suppressing vibration of a vibration platform may be created. It is obvious that the development of a relationship for deformation of the rod with nonlinear constitutive relations is the central role in control systems. For such a purpose, we assume that the rod has one fixed end (lower end) and a free end (top end) at which the pre-compression stress is specified. Denote the length of the rod by L , the longitudinal coordinate by x where the

original point is at the fixed end, and the local longitudinal displacement by $u = u(x)$. Then we have the longitudinal strain ε , related to the displacement in the form

$$\varepsilon = \frac{du}{dx} \quad (2.1)$$

The experimental investigation exhibits that this deformation is dependent on the local stress and magnetic field (see in Fig. 1), which is fully described by the following nonlinear constitutive model expressed by analytical formulae (Zheng and Liu, 2005)

$$\varepsilon = \frac{\sigma}{E_s} + \begin{cases} \lambda_s \tanh \frac{\sigma}{\sigma_s} + \left(1 - \tanh \frac{\sigma}{\sigma_s}\right) \frac{\lambda_s}{M_s^2} M^2 & \frac{\sigma}{\sigma_s} \geq 0 \\ \frac{\lambda_s}{2} \tanh \frac{2\sigma}{\sigma_s} + \left(1 - \frac{1}{2} \tanh \frac{2\sigma}{\sigma_s}\right) \frac{\lambda_s}{M_s^2} M^2 & \frac{\sigma}{\sigma_s} < 0 \end{cases} \quad (2.2)$$

$$H = \frac{1}{k} f^{-1}\left(\frac{M}{M_s}\right) - \begin{cases} 2\left[\sigma - \sigma_s \ln\left(\cosh \frac{\sigma}{\sigma_s}\right)\right] \frac{\lambda_s}{\mu_0 M_s^2} M & \frac{\sigma}{\sigma_s} \geq 0 \\ 2\left[\sigma - \frac{\sigma_s}{4} \ln\left(\cosh \frac{2\sigma}{\sigma_s}\right)\right] \frac{\lambda_s}{\mu_0 M_s^2} M & \frac{\sigma}{\sigma_s} < 0 \end{cases}$$

where σ represents the local stress in the rod; M and H are variables of the magnetization and magnetic field, respectively; E_0 and E_s are the initial and saturation Young's moduli, respectively; M_s indicates the saturation magnetization; λ_s stands for the saturation magnetostrictive coefficient; $\mu_0 = 4\pi \cdot 10^{-7}$ H/m is the magnetic permeability of vacuum; $f(y) = \coth(y) - 1/y$; $k = 3\chi_m/M_s$ represents the relaxation factor, where χ_m is the linear magnetic susceptibility; and $\sigma_s = \lambda_s E_s E_0 / (E_s - E_0)$.

Now, we rewrite Eq. (2.2)₁ in the prevalent form

$$\varepsilon = \frac{\sigma}{E(\sigma)} + \lambda(\sigma, H) \quad (2.3)$$

in which the nonlinear functions $E(\sigma)$ and $\lambda(\sigma, H)$ are respectively expressed as

$$\frac{\sigma}{E(\sigma)} = \frac{\sigma}{E_s} + \begin{cases} \lambda_s \tanh \frac{\sigma}{\sigma_s} & \frac{\sigma}{\sigma_s} \geq 0 \\ \frac{\lambda_s}{2} \tanh \frac{2\sigma}{\sigma_s} & \frac{\sigma}{\sigma_s} < 0 \end{cases} \tag{2.4}$$

$$\lambda(\sigma, H) = \begin{cases} \left(1 - \tanh \frac{\sigma}{\sigma_s}\right) \frac{\lambda_s}{M_s^2} M^2 & \frac{\sigma}{\sigma_s} \geq 0 \\ \left(1 - \frac{1}{2} \tanh \frac{2\sigma}{\sigma_s}\right) \frac{\lambda_s}{M_s^2} M^2 & \frac{\sigma}{\sigma_s} < 0 \end{cases}$$

When the applied magnetic field H is specified, we can get a dependence for M in terms of σ . Substituting the resulting dependence for $M = M(\sigma)$ into Eq. (2.4)₁, we can get a relation for $E = E(\sigma)$ which exhibits variable Young’s modulus as shown in Fig. 2. Equation (2.4)₂ presents the nonlinear part that is mainly relevant to the magnetostrictive deformation.

In the linearized constitutive model of the Terfenol-D rod, Eqs. (2.2) can be simplified into

$$\varepsilon = \frac{\sigma}{E} + dH \qquad B = d\sigma + \mu^0 H \tag{2.5}$$

where E is constant at a specific magnetic field; d represents the material constant; B stands for the magnetic flux density; and μ^0 is the magnetic permeability at a specific stress.

For the control system, the magnetic field H consists of two parts – one is the bias magnetic field and the other is the controlling magnetic field generated by a solenoid. In this case, we have

$$H(t) = c_0 I(t) + H_{bias} \tag{2.6}$$

Here, c_0 is the so-called coil factor, $I(t)$ stands for the time-variable control current in the solenoid, and H_{bias} indicates the bias applied magnetic field.

From the knowledge of electromagnetic fields, we know that the generated magnetic field in the solenoid can be formulated by Zhao and Chen (1995)

$$H_0(x, t) = \frac{nI(x, t)}{2} \left(\frac{x + l/2}{\sqrt{R^2 + (x + l/2)^2}} - \frac{x - l/2}{\sqrt{R^2 + (x - l/2)^2}} \right) \tag{2.7}$$

in which l and R represent the length and radius of the solenoid, respectively; and n stands for the coil number per unit length. When l is sufficiently larger than L , the distribution of the magnetic field in the solenoid is almost uniform. In this case, Eq. (2.7) can be simplified into the form

$$H_0(t) = \frac{nI(t)}{2} \frac{l}{\sqrt{R^2 + (l/2)^2}} = c_0 I(t) \tag{2.8}$$

Here

$$c_0 = \frac{nl}{2\sqrt{R^2 + (l/2)^2}}$$

In order to suppress the displacement vibration at the free end ($x = L$) of the rod, a closed loop control with a control law of negative displacement and velocity feedback is employed

$$I(t) = -G_1 u_f(t) - G_2 \dot{u}_f(t) \quad (2.9)$$

where $u_f(t)$ and $\dot{u}_f(t)$ are respectively the displacement and velocity signals at the free end of the rod, which can be detected by some sensing technique without difficulty; and G_1 and G_2 are the gains. Substitution of Eq. (2.9) into Eq. (2.6) leads to an expression for the applied magnetic field dependent on the displacement of the free end of the rod, i.e.,

$$H(t) = -c_0 G_1 u_f(t) - c_0 G_2 \dot{u}_f(t) + H_{bias} \quad (2.10)$$

To give a prediction for the displacement at the free end of the rod, the finite element method is utilized here. Denote the longitudinal distributed force by $F = F(x)$, which may be relevant to either a specific distribution or the magnetic force or both. From the deformation theory of rods, we know that the differential equation for the rod extension or contraction can be written as

$$\frac{\partial \sigma}{\partial x} + F - \rho \frac{\partial^2 u}{\partial t^2} - \eta \frac{\partial u}{\partial t} = 0 \quad (2.11)$$

associated with the boundary conditions of $u(0, t) = 0$, and $u(L, t) = u_0$. Here, $u_0 = u(H_{bias}, \sigma_0)$ is a displacement at the free end of the rod at the initial instant, ρ is the mass density per length of the rod, and η denotes the damping coefficient. By means of the weighted residual method, we get an equivalent integral form of Eq. (2.11) as follows

$$\int_V \delta u \left(\frac{\partial \sigma}{\partial x} + F - \rho \frac{\partial^2 u}{\partial t^2} - \eta \frac{\partial u}{\partial t} \right) dV = 0 \quad (2.12)$$

Here, δu represents a selected weighted residual function. Divide the length of the rod into K elements. Selecting the Lagrange interpolation polynomial functions $N_i(x)$ to approximately formulate the displacement in each element by means of the nod displacements, we have

$$u(x, t) = \sum_{i=1}^K N_i(x) u_i(t) = \mathbf{N}(x) \mathbf{u}(t) \quad (2.13)$$

Here,

$$\mathbf{N} = [N_1, N_2, \dots, N_K] \quad \mathbf{u} = [u_1, u_2, \dots, u_K]^T \quad (2.14)$$

Then we get a system of ordinary differential equations of the dynamic system in the matrix form

$$\mathbf{M}\ddot{\mathbf{u}}(t) + \mathbf{C}\dot{\mathbf{u}}(t) + \mathbf{K}(\sigma)\mathbf{u}(t) = \mathbf{Q}(t, \sigma, u_f(t), \dot{u}_f(t)) \quad (2.15)$$

Here, \mathbf{u} , $\dot{\mathbf{u}}$, and $\ddot{\mathbf{u}}$ are respectively the columns of node displacement, velocity, and acceleration; \mathbf{M} , \mathbf{C} and \mathbf{K} indicate the global matrices of mass, damping, and stiffness, respectively; $u_f(t) = u(L, t)$; and \mathbf{Q} represents the control force column. Their elements are explicitly formulated by

$$\begin{aligned} M^e &= \int_0^l \rho N^T N \, dx & K^e &= \int_0^l \frac{dN^T}{dx} E(\sigma) \frac{dN}{dx} \, dx \\ Q^e &= \int_0^l \frac{dN^T}{dx} E(\sigma) \lambda(\sigma, H) \, dx + P_j & & \begin{cases} P_j \neq 0 & \text{for } j = n_e \\ P_j = 0 & \text{for } j \neq n_e \end{cases} \end{aligned} \quad (2.16)$$

in which n_e indicates the node number. For the damping matrix, the Rayleigh damping is used here, i.e., \mathbf{C} is a linear combination of \mathbf{M} and \mathbf{K} . It is obvious that for the case of the linear constitutive model of magnetostrictive deformation (see Eqs. (2.5)), dynamic equations (2.15) for the control system become linear too. This entail that \mathbf{K} is independent of σ and \mathbf{Q} linearly changes with H . For the case of the nonlinear constitutive model, however, the dynamic equations are inherently nonlinear.

3. Numerical approach

In order to realize numerical simulations of the nonlinear control system, the essential step is to solve the nonlinear dynamic equations in the proposed theory. Once the quantities are obtained at a specific time instant t , Eq. (2.15) in the next time instant $t + \Delta t$, where Δt means a time step, can be formulated by Newmark's method

$$\mathbf{M}\ddot{\mathbf{u}}_{t+\Delta t} + \mathbf{C}\dot{\mathbf{u}}_{t+\Delta t} + \mathbf{K}(\sigma_{t+\Delta t})\mathbf{u}_{t+\Delta t} = \mathbf{Q}(\sigma_{t+\Delta t}, u_{f,t+\Delta t}, \dot{u}_{f,t+\Delta t}) \quad (3.1)$$

in which

$$\dot{\mathbf{u}}_{t+\Delta t} = \dot{\mathbf{u}}_t + [(1 - \delta)\ddot{\mathbf{u}}_t + \delta\ddot{\mathbf{u}}_{t+\Delta t}]\Delta t \quad (3.2)$$

$$\mathbf{u}_{t+\Delta t} = \mathbf{u}_t + \dot{\mathbf{u}}_t\Delta t + \left[\left(\frac{1}{2} - \alpha \right) \ddot{\mathbf{u}}_t + \alpha\ddot{\mathbf{u}}_{t+\Delta t} \right] \Delta t^2$$

From Eq. (3.2)₂, we get

$$\ddot{\mathbf{u}}_{t+\Delta t} = \frac{1}{\alpha\Delta t^2}(\mathbf{u}_{t+\Delta t} - \mathbf{u}_t) - \frac{1}{\alpha\Delta t}\dot{\mathbf{u}}_t - \left(\frac{1}{2\alpha} - 1\right)\ddot{\mathbf{u}}_t \quad (3.3)$$

Substituting Eq. (3.3) into Eq. (3.2)₁, and the resulting equation associated with Eq. (3.3) into Eq. (3.1), we have

$$\widehat{\mathbf{K}}_{t+\Delta t}\mathbf{u}_{t+\Delta t} = \widehat{\mathbf{Q}}_{t+\Delta t} \quad (3.4)$$

in which

$$\widehat{\mathbf{K}}_{t+\Delta t} = \mathbf{K}(\sigma_{t+\Delta t}) + d_0\mathbf{M} + d_1\mathbf{C} \quad (3.5)$$

$$\widehat{\mathbf{Q}}_{t+\Delta t} = \mathbf{Q}_{t+\Delta t} + \mathbf{M}(d_0\mathbf{u}_t + d_2\dot{\mathbf{u}}_t + d_3\ddot{\mathbf{u}}_t) + \mathbf{C}(d_1\mathbf{u}_t + d_4\dot{\mathbf{u}}_t + d_5\ddot{\mathbf{u}}_t)$$

where $d_0 = 1/(\alpha\Delta t^2)$, $d_1 = \delta/(\alpha\Delta t)$, $d_2 = 1/(\alpha\Delta t)$, $d_3 = 1/(2\alpha) - 1$, $d_4 = \delta/\alpha - 1$, $d_5 = (\delta/\alpha - 2)\Delta t/2$, $d_6 = (1 - \delta)\Delta t$, and $d_7 = \delta\Delta t$. Here, the parameters of δ and α in our simulations are taken as $\delta = 0.5$, $\alpha = 0.25$.

For the nonlinear constitutive model of the materials, it is known that the local internal stress is nonlinearly related to the deformation, expressed by Eq. (2.1), by means of the constitutive model described by Eqs. (2.2) at each time step, which yields nonlinear relations for $\mathbf{K}(\sigma_{t+\Delta t})$ and $\mathbf{Q}(\sigma_{t+\Delta t}, u_{f,t+\Delta t}, \dot{u}_{f,t+\Delta t})$ varying with $\mathbf{u}_{t+\Delta t}$ at the time step $t + \Delta t$. In order to solve this nonlinearity, an incremental iterative approach is employed here. That is to say, we substitute the initial iterative value of $\mathbf{u}_{t+\Delta t}$ by $\mathbf{u}_{t+\Delta t}^{(0)} = \mathbf{u}_t$. Then the internal stress σ can be found from Eqs. (2.1) and (2.2) for the applied magnetic field at the instant $t + \Delta t$. Substituting the resulting internal stress into Eq. (3.4), we get an iterated displacement of this instant. Replacing the iterated displacement by the previously found displacement, and repeating this iterative approach, we obtain the displacement of the rod at the instant $t + \Delta t$ till the following condition is satisfied

$$\left\| \frac{\sigma_{t+\Delta t}^{(j+1)} - \sigma_{t+\Delta t}^{(j)}}{\sigma_{t+\Delta t}^{(j)}} \right\| < \delta_1 \quad \text{and} \quad \left\| \frac{\mathbf{u}_{t+\Delta t}^{(j+1)} - \mathbf{u}_{t+\Delta t}^{(j)}}{\mathbf{u}_{t+\Delta t}^{(j)}} \right\| < \delta_2 \quad (3.6)$$

Here, the superscript j represents the iteration step, while δ_1 and δ_2 are the pre-selected accuracies. In the following simulations, we take $\Delta t = 1 \cdot 10^{-6}$, and $\delta_1 = 1 \cdot 10^{-6}$, $\delta_2 = 1 \cdot 10^{-4}$.

4. Numerical results and discussions

In order to present the efficiency of the nonlinear control system proposed here, the following geometric and material parameters are assumed in the simulations

$$\begin{array}{lll}
 L = 114.5 \text{ mm} & D = 38.1 \text{ mm} & \rho = 9130 \text{ kg/m}^3 \\
 \lambda_s = 1300 \text{ ppm} & \chi_m = 80 & \mu_0 M_s = 0.8 \text{ T} \\
 E_s = 110 \text{ GPa} & \sigma_s = 200 \text{ MPa} & c_0 = 9488.49
 \end{array}$$

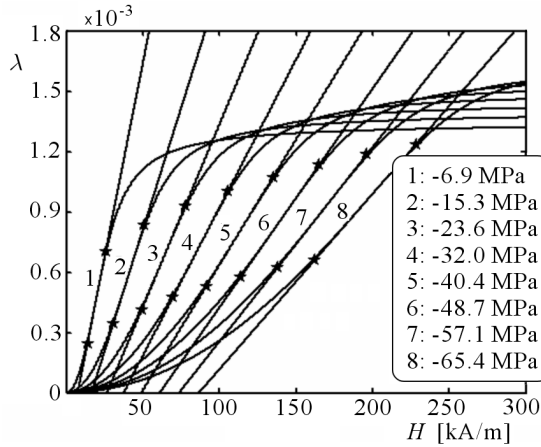


Fig. 4. Curves of magnetostrictive strain versus the applied magnetic field for different constant stresses; straight lines: linearized constitutive model (Moffet *et al.*, 1991); curve lines: nonlinear constitutive model (Zheng and Liu, 2005)

Before we disclose results of the simulations of the dynamic control carried out on the basis of the nonlinear constitutive model (Zheng and Liu, 2005), let us see the suitability of the similar control system to the approximate linear constitutive model (or Eqs. (2.5)). In practical applications, the Terfenol-D based actuators (see Fig. 3) have built-in adjustable pre-stress to place the material on the almost linear region of magnetostrictive curves by a permanent magnet or an offset coil to generate a bias magnetic field. After that, the gains in the feedback loop are optimally selected in the stability region of the control. According to the experiment by Moffet *et al.* (1991), we can get the bias magnetic field dependent on the pre-stress at the middle of the approximately linear region (see Table 1 for eight sets of different compressive pre-stresses). Then we can plot the linear curves of strain(λ)-field(H) to compare them with the nonlinear curves of the corresponding relation as shown in Fig. 4.

From this figure, one can see that the linear region is suitable only in a narrow area indicated by the asterisks in each curve of the figure. For example, the bias magnetic field is valid in the region of (30.72,51.03) kA/m for the linear model when the pre-stress is -15.3 MPa. Since the constitutive model of the material is inherently nonlinear, in fact we still get nonlinear relations between the magnetostrictive strain and the stress even when the linear relation is used. This is shown in Fig. 5 where the characteristic $E = E(\sigma, H)$ in the nonlinear constitutive model is employed. This result tells us that the control system should be nonlinear even when the linear constitutive model is used. This nonlinear effect, however, is neglected in design of control systems based on linear models, which leads to some deviation in practical realisation of the control goal.

Table 1. Numerical results of the bias magnetic field relevant to pre-stress (Moffet *et al.*, 1991)

| Bias condition | 1 | 2 | 3 | 4 | 5 | 6 | 7 | 8 |
|------------------------------|-------|-------|-------|-------|--------|--------|--------|--------|
| Compressive pre-stress [MPa] | 6.9 | 15.3 | 23.6 | 32.0 | 40.4 | 48.7 | 57.1 | 65.4 |
| Magnetic bias field [kA/m] | 11.94 | 31.83 | 55.70 | 79.58 | 103.45 | 127.32 | 151.20 | 175.07 |

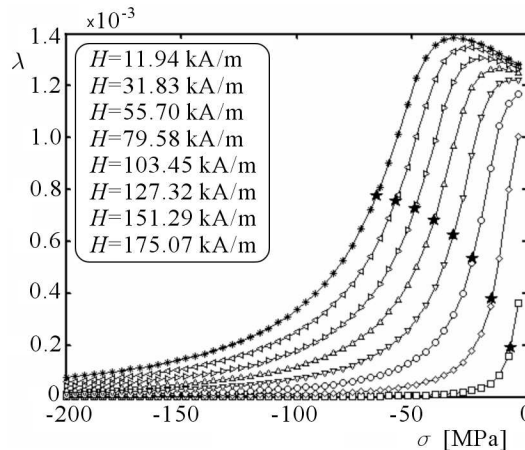


Fig. 5. Curves of magnetostrictive strain versus internal stress of the rod for different constant magnetic fields

As a case study without losing generality, we present simulations of the dynamic control system with the nonlinear constitutive model when the pre-stress is -15.3 MPa, and compare then with those of the system based on

the linear model. Here, the initial deviation of displacement is utilized and the gains of the feedback loop are taken as $G_1 = 0$, and $G_2 = 0.84$ in all simulations. Firstly, we present the results of the control system when the point of the bias magnetic field is located at the middle of the straight line of the $\lambda \sim H$ relation, where the bias magnetic field is equal to 31.83 kA/m.

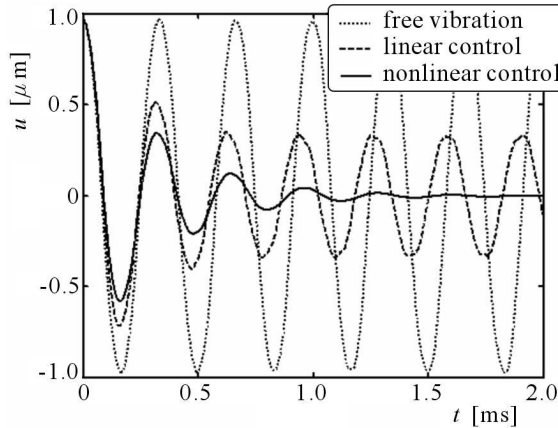


Fig. 6. Comparison of simulation results of the dynamic control between systems based on the nonlinear constitutive model and its linearized version when the bias magnetic field is taken at the middle of the suitable region of the latter model, i.e. when the pre-stress is -15.3 MPa and the bias magnetic field is selected at 31.83 kA/m

Figure 6 plots time responses of displacement at the free end of the rod for three cases: free vibration without control, active control with either the nonlinear or linear model. From this figure, we find that the displacement vibration may be fully suppressed during of about 1.0 ms for the nonlinear control system proposed, while the vibration in the linear control model is slowly attenuated after 0.5 ms and the duration is much longer than 2.0 ms, as shown in this figure. When the bias magnetic field is taken out of the suitable region, i.e. either $H_{bias} = 15.92$ kA/m or 63.66 kA/m, Figs. 7 and 8 show the simulation results in such a case. From these two figures, we know that the control based on the linear model loses its stability for some selected bias magnetic fields, while the displacement vibrations are still suppressed during the duration of about 1.0 ms for the nonlinear control proposed here. These notable deviations between the control strategies based on the nonlinear and linear models of the Terfenol-D rod indicate that the nonlinear control should be preferred in practice since the nonlinear constitutive model is more close to the real case.

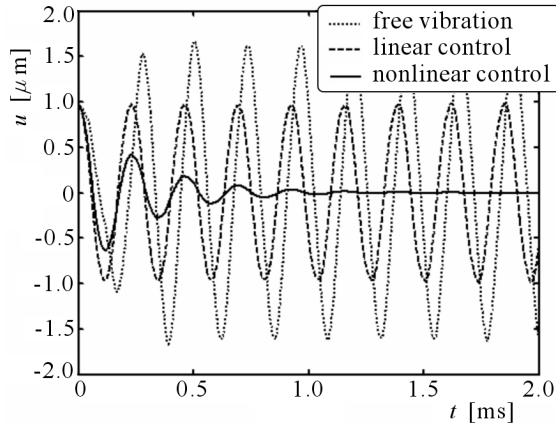


Fig. 7. Comparison of simulation results of the dynamic control between systems based on the nonlinear constitutive model and its linearized version when the bias magnetic field is taken at one edge of the suitable region of the latter model, i.e. when the pre-stress is -15.3 MPa and the bias magnetic field is selected at 15.92 kOe

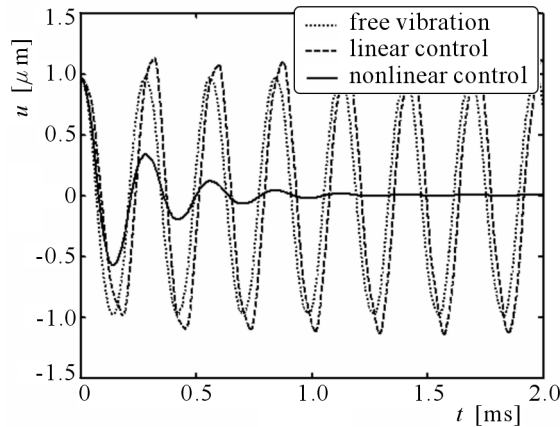


Fig. 8. Comparison of simulation results of the dynamic control between systems based on the nonlinear constitutive model and its linearized version when the bias magnetic field is taken out of the suitable region of the latter model, i.e. when the pre-stress is -15.3 MPa and the bias magnetic field is selected at 63.66 kOe

5. Conclusions

A simulation model of the control system of the Terfenol-D transducer is proposed on the basis of analytical formulae of the nonlinear constitutive model

of the materials used. The numerical results for the analyzed case study of the control system exhibit that the nonlinear control is efficient in suppressing displacement vibrations at the free end of the rod. Comparing the results with corresponding control simulations based on the linearized constitutive model, we find that the linear control design is effective only when the point of the bias magnetic field is located in a small region of the linearized area around the middle point of the region. The nonlinear control design is more efficient than the linear control strategy in this small region. When the bias magnetic field is close to the edge of the linear area or outside of it, however, the nonlinear control still remains efficient, but the linear method loses its stability.

Acknowledgement

This work was supported by the Fund of Natural Science Foundation of China (No. 10132010, 90405005, 10025205), the Fund of Ministry of Education of China for the Research Team in New Century and the Science Foundation of the Ministry of Education of China for Ph. D program. The authors gratefully acknowledge these supports.

References

1. BARTLETT P.A., EATON S.J., GORE J., METHERINGHAM W.J., JENNER A.G., 2001, High power low frequency magnetostrictive actuation for anti-vibration applications, *Sensors and Actuators A*, **91**, 133-136
2. CARMAN G.P., MITROVIC M., 1995, Nonlinear constitutive relations for magnetostrictive materials with application to 1-D problems, *J. Intell. Mater. Syst. Struct.*, **6**, 673-683
3. DUENAS T., HSU L., CARMAN G.P., 1996, Magnetostrictive composite material systems analytical/experimental (Invited paper), In: *Advances in Materials for Smart Systems Fundamental and Applications*, Materials Research Society Symposium, Boston
4. FLATAU A.B., HALL D.L., 1992, Magnetostrictive vibration control system, *The 30th Aerospace Science Meeting and Exhibit*, Reno, Nevada, USA
5. HILLER M.W., BRYANT M.D., UMEGAKI J., 1989, Attenuation and transformation of vibration through active control of magnetostrictive Terfenol, *Journal of Sound and Vibration*, **134**, 507-519
6. JENNER A.G., GREENOUGH R.D., ALLWOOD D., WILKINSON A.J., 1994, Control of Terfenol-D under load, *Journal of Applied Physics*, **78**, 7160-7162

7. MOFFET M.B., CLARK A.E., WUN-FOGLE M., LINBERG J., TETER J.P., McLAUGHLIN E.A., 1991, Characterization of Terfenol-D for magnetostrictive transducers, *J. Acoust. Soc. Am.*, **89**, 3, 1448-1455
8. NAKAMURA Y., NAKAYAMA M., MASUDA K., 2000, Development of active six-degrees-of-freedom microvibration control system using giant magnetostrictive actuators, *Smart Materials and Structures*, **9**, 175-185
9. PAGLIARULO P., KUHNEN K., MAY C., JANOCIA1 H., 2004, Tunable magnetostrictive dynamic vibration absorber, *Proceedings of the 9th International Conference on New Actuators*, Bremen, Germany, 367-370
10. REED R.S., 1988, Active vibration isolation using a magnetostrictive actuator, *Modeling and Simulation*, **19**
11. ZHANG C.L., MEI D.Q., CHEN Z.C., 2003, Fuzzy generalized predictive control of microvibration for a micro-manufacturing platform, *Proceedings of the American Control Conference*, Denver, Colorado, USA, 3690-3695
12. ZHANG T.L., JIANG C.B., ZHANG H., XU H.B., 2004, Giant magnetostrictive actuators for active vibration control, *Smart Materials and Structures*, **13**, 473-477
13. ZHAO K.H., CHEN X.M., 1995, *Electromagnetics*, Higher Education Publications, Beijing [in Chinese]
14. ZHENG X.J., LIU X.E., 2005, A nonlinear constitutive model for Terfenol-D rods, *Journal of Applied Physics*, **97**, 053901

**Aktywne sterowanie drganiami w wielkim akuatorze
magnetostrykcyjnym z rdzeniem typu Terfenol-D przy uwzględnieniu
nieliniowych równań konstytutywnych**

Streszczenie

W pracy zaprezentowano symulacje numeryczne aktywnego sterowania za pomocą wielkiego akuatora magnetostrykcyjnego zawierającego rdzeń wykonany z Terfenolu-D opisanego nieliniowymi zależnościami konstytutywnymi. Celem rozważań jest analiza tłumienia drgań swobodnego końca pręta, zwykle łączonego z platformą. Wydłużenie pręta jest opisane nieliniowym równaniem z powodu nieliniowych relacji pomiędzy przykładanym polem magnetycznym, naprężeniami wstępnymi oraz odkształceniami. Po sformułowaniu przez ostatniego Autora niniejszej pracy modelu pręta z Terfenolu-D oraz zastosowaniu metody elementów skończonych, wprowadzono procedurę numeryczną o symulacji dynamiki układu sterowania z ujemnym sprzężeniem zwrotnym ze względu na przemieszczenie i prędkość końca akuatora. Wyniki badań pokazały, że tego typu sterowanie staje się bardziej efektywne niż inne strategie redukcji drgań oparte na modelach liniowych.

Manuscript received February 21, 2007; accepted for print April 4, 2007